28

Discovery of Protein Kinase Phosphatase Inhibitors

Andreas Vogt and John S. Lazo

Summary

Dynamic protein phosphorylation, a major cellular regulatory system, is tightly controlled by coordinating the reversible action of protein kinases and phosphatases. Recent evidence is consistent with sophisticated mechanisms that regulate both kinases and phosphatases in the cell. Dual specificity phosphatases, which act on phosphorylated serine, threonine, and tyrosine residues in proteins, are valid targets for drug discovery. Chemical complementation combines genetic manipulations with chemical biology and high-content multiparametric analyses and was developed as a screening approach to discover protein phosphatase inhibitors. Using a dual specificity mitogen-activated protein kinase phosphatase as an example, a detailed protocol, discussion of issues relating to data analysis, and high-throughput implementation of the chemical complementation approach to drug discovery is presented.

Key Words: DSPases; high content screening; inhibitors; Kolmogorov–Smirnov statistics; MKP-1; sanguinarine.

1. Introduction

After synthesis, approximately one-third of mammalian proteins are phosphorylated ***(1)***. Dynamic protein phosphorylation is one of the major mechanisms by which cells regulate transcription, signal transduction, motility, death and survival, and metabolism. The phosphorylation status of cellular proteins is tightly controlled by the concerted and reversible action of kinases and phosphatases. Although the importance of protein kinases has long been recognized, a growing body of evidence now demonstrates that the regulation of protein phosphorylation at the level of the protein phosphatases is as sophisticated as that mediated by the protein kinases (reviewed in **ref.** *2*). Based on the preference of certain phosphatases for one phosphorylated hydroxy amino acid over others, protein phosphatases historically have been classified as serine/threonine specific (STPase), tyrosine-specific (PTPases), and dual-specific (DSPases) phosphatases; more recently structural information has been used to refine the classification scheme ***(3)***. Although a number of potent and selective inhibitors of STPases have been isolated from natural sources, selective PTPase or DSPase inhibitors are still rare. Although genetic approaches using inhibitory RNA can provide some insight into the functionality of these phosphatases, at least some of the PTPases and DSPases interact with other proteins and regulate their function in a manner that is independent of their phosphatase activity (e.g., *see* **ref.** *4*). Therefore, potent and selective small molecule inhibitors of phosphatase activity would be quite valuable to probe the biochemical substrates and functionality of protein phosphatases under conditions of acute and reversible inhibition. However, the discovery of small molecule inhibitors of protein phosphatases has been challenging for a variety of reasons.

From: *Methods in Molecular Biology, vol. 356:*
High Content Screening: A Powerful Approach to Systems Cell Biology and Drug Discovery
Edited by: D. L. Taylor, J. R. Haskins, and K. Giuliano © Humana Press, Inc., Totowa, NJ

Currently, the most popular approach to identifying potential phosphatase inhibitors are in vitro assays using recombinant enzymes; however, some phosphatases are difficult to produce in pure and active form using recombinant DNA technology *(5)*. In the case of mitogen-activated kinase phosphatase (MKP)-1, for instance, the unavailability of large amounts of recombinant enzyme has prevented large-scale screening and has impeded structural studies. In those cases in which active phosphatases are available, the assays typically employ small molecule synthetic substrates, such as para-nitrophenyl phosphate or *O*-methyl fluorescein phosphate. These small molecule substrates have been employed because they provide a robust output signal, are inexpensive, and are more convenient to use than the phosphorylated protein substrate. Nonetheless, we now know that the activity of many protein phosphatases depends on their interaction with other proteins in the cell *(6,7)* and thus, in vitro screening assays might not be predictive of compound effect within the context of the whole cell *(8)*.

Cell-based assays could provide a solution to this dilemma as the cell provides the proper and complete environment for enzymatic activity. Measurement of protein substrate phosphorylation levels can be used as a readout, although steady state phosphorylation levels reflect the relative activity of both kinases and phosphatases. Thus, measurements of protein phosphorylation of extracellular signal-regulated kinase (Erk), a target for MKPs and Cdc25A, have been used to identify cell-active inhibitors of the dual-specificity phosphatases Cdc25 and MKP-3 *(9)*. As anticipated, however, such screens also identified many compounds that do not affect phosphatase activity. Multiparameter high-content analysis has allowed us to develop a more definitive phosphatase assay in intact mammalian cells. In the following section, we provide the reader with a detailed discussion of a powerful new method, which we have termed "chemical complementation" *(10,11)*. Although the assay, in principle, should be applicable to any phosphatase (or kinase) whose cellular substrate is known, we have focused on dual specificity phosphatases, in particular MKPs because of their potential roles in human disease and the dearth of small molecule inhibitors.

1.1. Chemical Complementation: A Novel Cellular Assay to Detect Phosphatase Inhibition in Intact Cells

Chemical complementation combines the certitude of genetic manipulations with the power of chemical biology and high content, multiparametric cellular analyses. The assay is based on measurement of protein phosphorylation in cell populations induced to overexpress the target phosphatase of interest (indicated by green [shaded] cells in **Fig. 1**). Phosphorylation levels of a known phosphatase target are visualized in individual cells by immunofluorescence, resulting in a low-phosphorylation phenotype in phosphatase-expressing cells, and a high-phosphorylation phenotype in nonexpressing cells (indicated in **Fig. 1** by red [dark] nuclei). Differences in phosphorylation levels between the two cell subpopulations then become a measure of phosphatase activity within the cell. In phosphatase-transfected cell populations not treated with inhibitors, phosphorylation differences would be expected to be large. Inclusion of a phosphatase inhibitor should reduce these differences. **Figure 2A** illustrates the differential phosphorylation phenotype for the three MKPs, MKP-1, MKP-3, and MKP-X. The differences in phosphorylation between expressing and nonexpressing cell populations are quantifiable (**Fig. 2B**), and the broad spectrum tyrosine phosphatase inhibitor, phenylarsine oxide (PAO) gradually reduces subpopulation differences to those observed with the phosphatase inactive green fluorescent protein (GFP) (**Fig. 2C**) *(9)*. The utility of the approach will be illustrated by a small-scale library screen for inhibitors of MKP-1, which resulted in the identification of the plant alkaloid, sanguinarine, as a selective inhibitor of MKP-1. The following sections provide the readership with a detailed protocol, a discussion of issues relating to data analysis and high-throughput implementation, and a graphical overview of the entire procedure (**Fig. 3**).

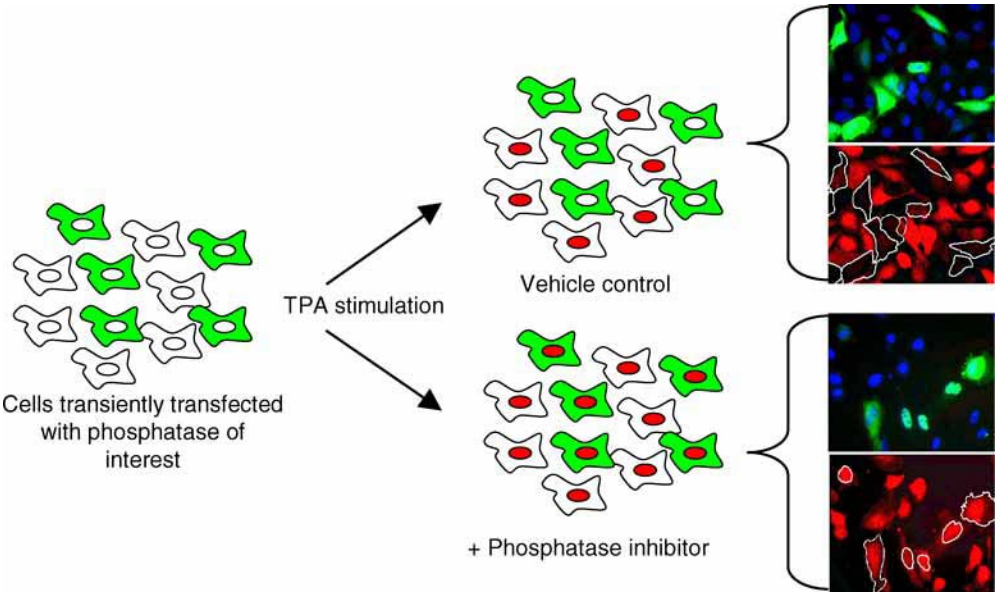

Fig. 1. A schematic figure of the principle of a high-content single cell chemical complementation assay. Cells are transfected with DNA encoding the molecular target of interest. Ectopic expression can either be transient or prolonged and target expression (shaded cells) is revealed by an epitope tag inserted into the target protein. The cells that are not expressing the target protein are used for internal controls. The phenotypic readout in this model is a phosphorylated protein located in the nucleus (dark nuclei). Expression of the targeted phosphatase suppresses phosphorylation and nuclear appearance. Inhibition of phosphatase activity with a small molecule results in a return of the normal phenotype and phosphorylation and nuclear presence of the substrate in target-expressing cells (traced in white). (Please *see* the companion CD for the color version of this figure.)

2. Materials

2.1. Transfection

1. HeLa cells (ATCC, Manassas, VA).
2. 384-well flat bottom micropates, collagen-coated (Falcon Biocoat).
3. Lipofectamine 2000 (Invitrogen, Carlsbad, CA; cat. no. 11668).
4. Plasmid encoding c-*myc*-tagged *mkp-1* in mammalian expression vector.
5. DMEM growth medium, supplemented with 10% fetal bovine serum and antibiotics.
6. Optimem reduced serum medium for transfection (GIBCO, Gaithersburg, MD; cat. no. 31985).

2.2. Treatment and Immunostaining

1. 0.2% Tween-20 (Sigma, cat. no. P-7949).
2. 0.2% Triton X-100 (Sigma, cat. no. T-9284).
3. Blocking solution: 21.68 mL 1X PBS, 820 µL BSA (Sigma, cat. no. A-0336), 2.5 mL goat serum (Chemicon, cat. no. S26). Filter through 0.2 µm syringe filter.
4. Primary antibody cocktail: anti-c*Myc* (Santa Cruz, cat. no. sc-40) anti-pErk (Cell Signaling, cat no. 9101, both at 1/200 dilution).
5. Secondary antibody cocktail: Alexa 488 goat antimouse IgG (fluorescein isothocyanate [FITC] equivalent; Molecular Probes), Alexa 555 goat antirabbit IgG (TRITC equivalent), Alexa 594 goat antirabbit IgG (Texas Red), or Alexa 647 goat antirabbit IgG (Cy5 equivalent) in blocking solution containing 1 µg/µL Hoechst 33342 (Molecular Probes, cat. no. A11029, A11037, A21245, and H-1399, respectively).
6. Formaldehyde: ultrapure formaldehyde 16% (Polysciences Inc., cat. no. 18814-20).
7. 12-*O*-tetradecanoylphorbol 13-acetate (TPA) (Sigma, cat. no. T-1585).
8. Test compounds as 200X DMSO stocks.

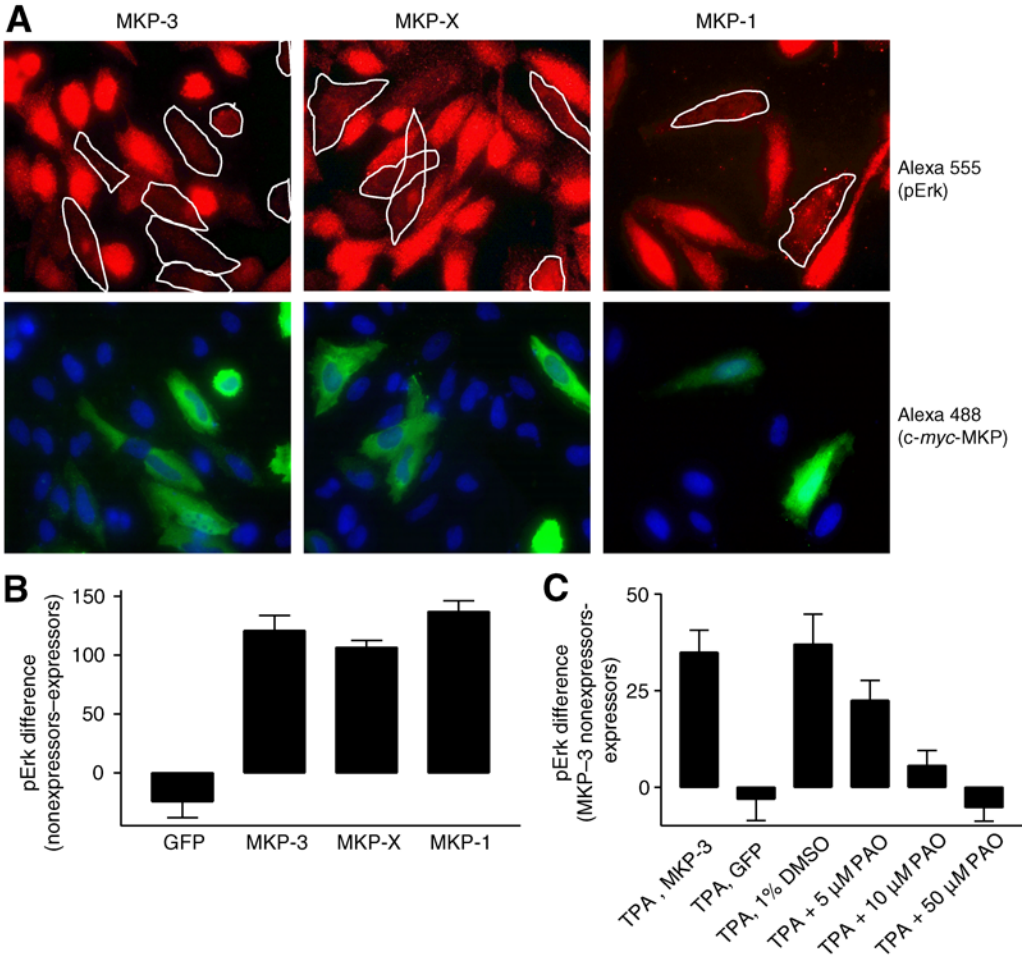

Fig. 2. Differences in target phosphorylation levels as a measure of phosphatase activity. **(A)** MKP-1, MKP-3, MKP-X phenotypes. **(B)** Quantification of phosphorylation differences in phosphatase expressing and nonexpressing cell subpopulations. **(C)** Concentration-dependent inhibition of MKP-3 by phenylarsine oxidase. (Please *see* the companion CD for the color version of this figure.)

2.3. Compounds

The MicroSource Natural Products Library (Discovery Systems, Inc., Gaylordsville, CT) is a 720 compound collection of pure natural products and their derivatives. Compounds were supplied as 10 m*M* stocks in DMSO, stored at –20°C, and thawed immediately before analysis. Aliquots were dissolved to a final concentration of 50 μ*M* in complete growth medium before cell treatment.

3. Methods

3.1. Cell Transfection, Treatment, and Processing

3.1.1. Day 1

Plate 5000 HeLa cells in the wells of a collagen-coated 384-well microplate.

3.1.2. Day 2

1. Transfect cells with c-*myc*-tagged *mkp-1* using Lipofectamine 2000 according to manufacturer's instructions. Use 100 ng DNA per well and a ratio of 2.5 μL Lipofectamine 2000 per μg of DNA (*see* **Note 1**).
2. Expose cells to DNA complexes for 3.5 h.
3. Replace transfection medium with complete growth medium and let cells recover overnight.

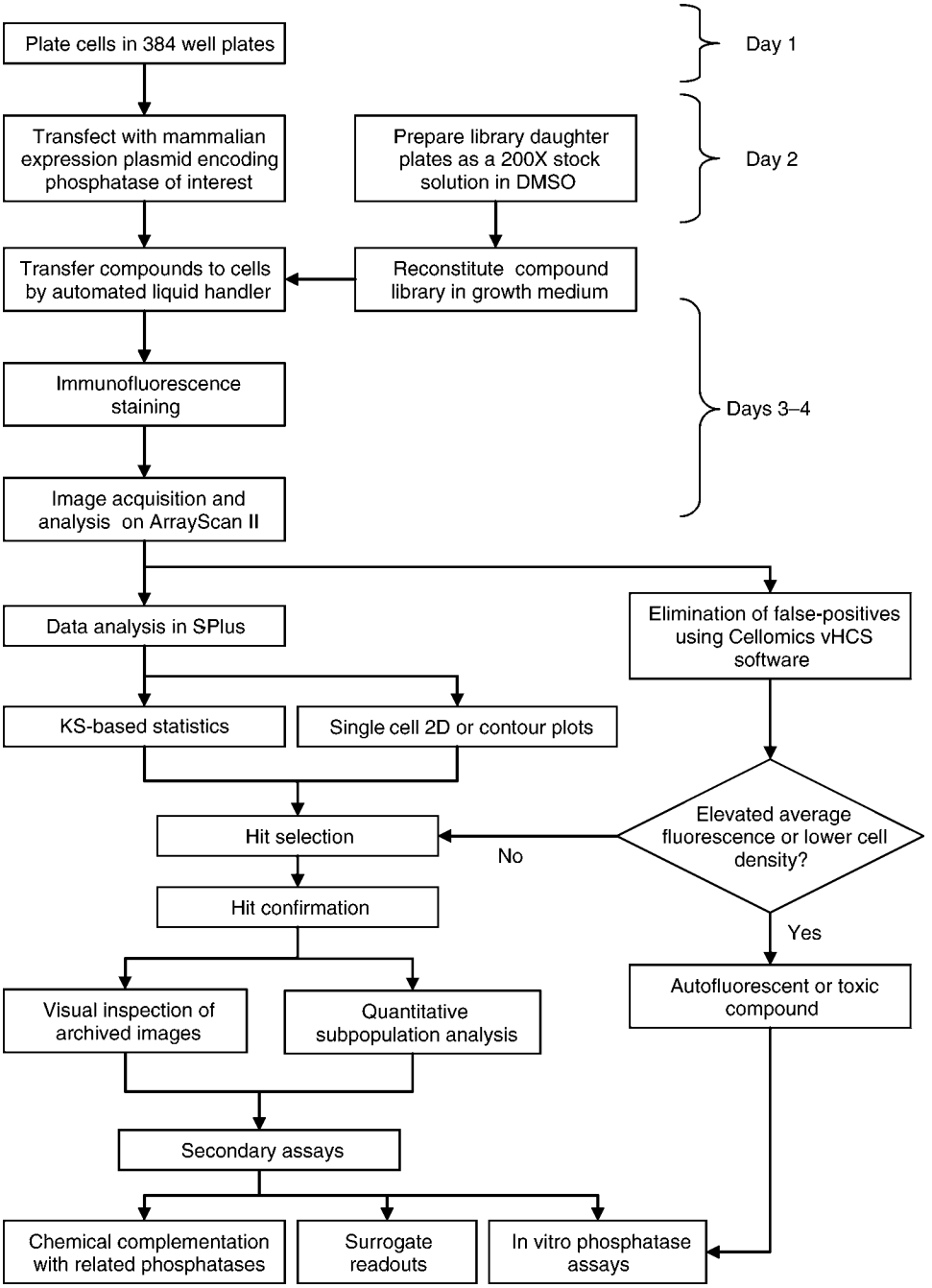

Fig. 3. Flow diagram of the chemical complementation procedure.

3.1.3. Day 3

1. Prepare 96-well treatment plates (clear polystyrene) containing 50 μL of compounds at the desired concentration in complete growth medium.
2. Treat cells with library compounds by transferring 30 μL of treatment solution from 96-well plates. A robotic liquid handler is necessary for this step.
3. Prepare 15 mL of 1.5 μg/μL TPA by adding 22.5 μL of 1 mg/mL DMSO stock of phorbol ester (TPA) in DMSO to 15 μL complete growth medium.

4. Dispense 15 mL TPA directly to cells from a single reservoir.
5. Return plates to incubator for 20 min.
6. Add 15 μL 16% formaldehyde directly to each well without removing medium and incubate at room temperature for 10 min.
7. Remove fixative and wash once with PBS.
8. Permeabilize for 5 min with Triton X-100.
9. Wash with PBS and incubate in blocking solution at room temperature for 1 h.
10. Remove blocking solution and incubate with primary antibody cocktail at room temperature for 1 h.
11. Remove primary antibody cocktail and incubate for 15 min with Tween-20.
12. Wash with PBS.
13. Incubate with secondary antibody cocktail for 1 h at room temperature in the dark.
14. Remove secondary antibody cocktail and incubate for 10 min with Tween-20.
15. Wash cells thrice with PBS, leaving last wash on cells.
16. Seal plate, and store at 4°C in the dark until analysis.
17. Add 60 μL PBS to each well, seal and barcode plate, and store at 4°C until needed for imaging.

3.2. Image Acquisition and Analysis

Immunostained plates were analyzed on the Cellomics, Inc., ArrayScan II using the Target Activation or Compartmental Analysis Bioapplication. Both algorithms are powerful image analysis tools that automatically set backgrounds, identify objects, and define regions of interest within the cells. Up to 100 readouts are provided for each cell, including fluorescence measurements, object counts, and nuclear morphology descriptors. Some of the features are ratiometric measurements.

For the chemical complementation screen, images were acquired in three independent fluorescence channels using an Omega XF93 filter set at excitation/emission wavelengths of 350/461 nm (Hoechst), 494/519 nm (AlexaFluor 488), 650/665 nm (AlexaFluor 647), respectively. The assay can be conducted using Texas red in place of Alexa 647, resulting in shorter exposure and screen times. Texas red compatible fluorophores require the use of an XF53 filter set. A nuclear mask was generated from Hoechst 33342-stained nuclei, and object identification thresholds and shape parameters were set such that the algorithm identified over 90% of the nuclei in each field. Objects that touched each other or the edge of the image were excluded from the analysis. The number of cells in each well was determined by enumerating objects in the Hoechst channel. At least 1000 individual cells were captured for each condition. For determination of MKP-1 and phospho-Erk expression levels, the nuclear mask was dilated by one pixel and AlexaFluor 488 and AlexaFluor 647 fluorescence intensities measured. The ArrayScan system in connection with Cellomics Store automatically archives images and plate data in a proprietary Structured Query Language (SQL) server database. Data and images are retrieved from the SQL database through a suite of HCS analysis algorithms termed the HCS toolbox.

3.3. HCS Data Set Evaluation

Average pixel intensities need to be evaluated for each individual cell to relate phospho-Erk levels to MKP-1 expression. Assuming that a minimum of 1000 cells are acquired in each well, a full 384-well plate will yield about 400,000 individual objects. This necessitates the use of non-Excel-based software, as Excel spreadsheets are limited to 65,000 objects. Our version of the Cellomics, Inc., software provides convenient well average readouts but is Excel-based and does not permit the export of all of the objects in the data set. Therefore, to perform the single-cell analysis, the individual cell-data was exported into the S-Plus statistical package (Insightful, Inc.) (*see* **Note 2**). Wells transfected with MKP-1 but not treated with compounds show low phospho-Erk signal in cells with high FITC signal. In the presence of a phosphatase inhibitor, many of the cells with high FITC signal become phospho-Erk positive. This increased density of phospho-Erk positive cells

at higher FITC intensities appears as a "filling" of the individual two dimensional (2D) plots. Visualization can be improved by generating density contour plots such as is shown in **Fig. 6A**.

3.3.1. Subpopulation Analysis

One method of quantifying the HCS data is based on the differential measurement of phospho-Erk levels in MKP-1 expressing and nonexpressing cell populations ***(9)***. Cell populations are gated into MKP-1 expressors and nonexpressors based on their average nuclear FITC intensity using S-plus scripts. The subsetting procedure can be automated by defining thresholds for FITC positive cells as the average FITC intensity of untransfected wells plus multiples of standard deviation. Cells are classified as "expressors" if their average FITC intensity exceeds this threshold. Alternatively, thresholds can be set manually (*see* **Note 3**). Once the data have been subsetted, phospho-Erk levels can be averaged in the two cell subpopulations as described ***(9)***. This method of evaluating the data set has been shown to be quantitative, but it is sensitive to outliers and shows extensive data scatter when used for screening. **Figure 4A** shows the results of the 720 member MicroSource natural products library screen using phospho-Erk subpopulation differences. The signal-to-noise ratio is low and positive controls (indicated by a dotted line) are not well separated from background, making it difficult to set a cutoff for identification of positives. Despite this, the method is still useful to confirm the activity of positives identified from HCS screens (*see* **Fig. 3**).

3.3.2. Kolmogorov–Smirnov Statistics

Because the algorithm described in **Subheading 3.3.1** lacked discriminating power as a high-throughput data evaluation tool, we developed an alternative method to identify compounds with phosphatase inhibitory activities based a two-dimensional Kolmogorov–Smirnov (2D KS) analysis ***(12)***. KS statistics are a method to quantitatively compare the distributions of individual cell populations ***(13–16)***, and were shown to be a valuable tool for the quantification of HCS data ***(17)***. The 2D KS method ranges over data in an (x,y) plane in search of a maximum cumulative difference between two 2D data distribution ***(18,19)***. The resulting KS values can assume a value between 0 (identical distributions) and 1 (completely different distributions). To fully exploit the information contained in our multiparameter high-content data, we developed ***(12)*** an algorithm that combined the KS statistics with ratio analysis of means ***(15)*** of both Alexa 488 (MKP-1) and Alexa 647 (phospho-Erk) in a minimum of 1000 individual cells in 192 wells on a 384-well microplate. Two-color fluorescence data from 16 controls (MKP-1 transfected but not drug treated wells) were pooled for each fluorescence channel and used to generate a 2D reference data distribution. The 2D data distribution of each individual well was then compared to the reference data distribution, and a KS value was calculated for each well. Calculations were performed with the S-Plus statistical software package. **Figure 4B** shows the results of the 720 member MicroSource natural products library 2DKS algorithm compared to the earlier-described subpopulation analysis. The algorithm dramatically reduced background noise and reduced the percentage of "hits" from 3% to a more manageable 0.7%.

3.3.3. False-Positives

False-positives are common in cell-based screens with fluorescent labels. Most false-positives fall into four categories: Toxicity (including morphological changes), autofluorescence, artifacts (from reagents or through outside contamination), and analysis abnormalities (such as out of focus wells). With phenotypic assays, we have found that the false-positive rate can be as high as 60% ***(9)***. An automated microscopy platform permits rapid and convenient identification of autofluorescence and toxicity through measurements of cell densities and well average fluorescence intensities. We have found that eliminating toxicity and fluorescence artifacts reduces the number of hits enough to permit evaluation of remaining positives by visual inspection of archived images. It should be noted that compounds should not be eliminated from consideration merely

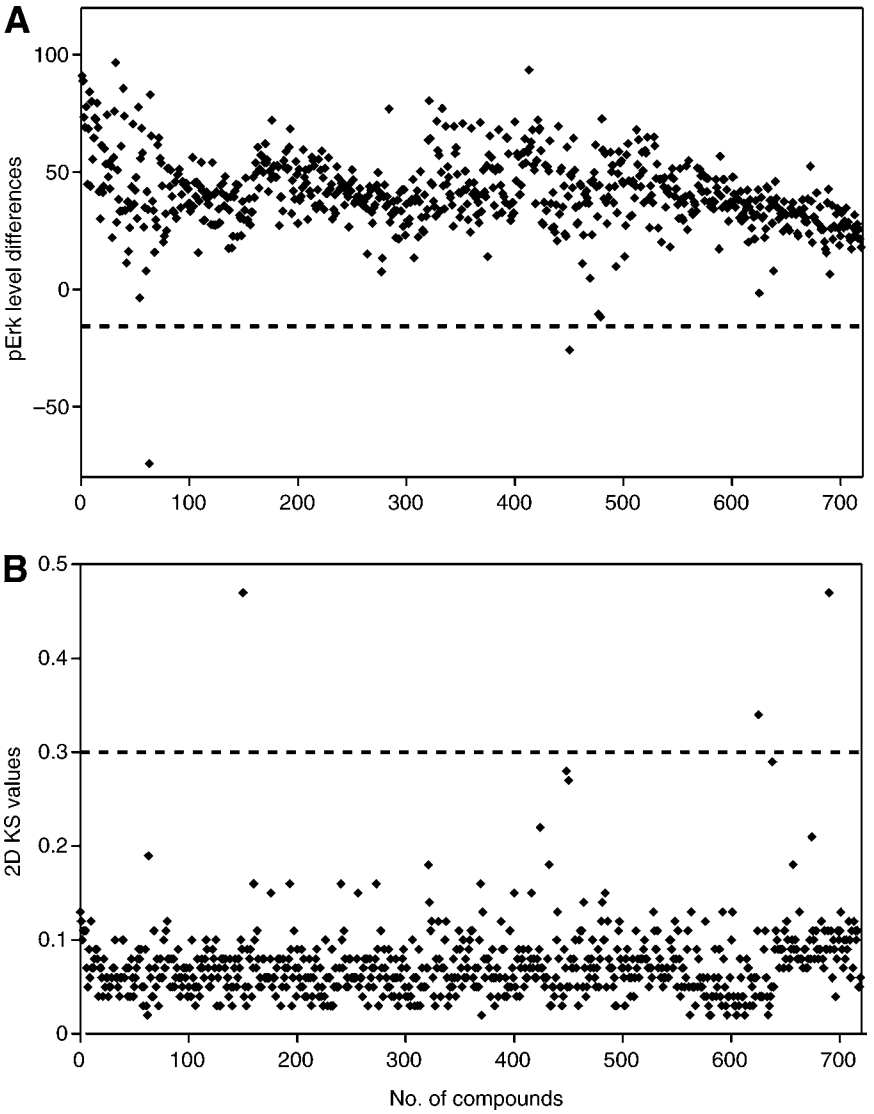

Fig. 4. Identifying hits in the chemical complementation assay by using subpopulation differences or 2D KS statistics. Differential expression of nuclear phospho-Erk was quantified in HeLa cells either transiently expressing or not expressing ectopic MKP-1. Cells were treated for 15 min with 0.5 μg/mL TPA in the presence or absence of compounds from a 720 member Microsource natural products library. **(A)** Represents the subpopulation difference in phospho-Erk levels. **(B)** Represents the 2D KS values for the entire cell population. Average pErk subpopulation differences or 2D KS values of wells treated with the positive control (PAO) are indicated by the dotted lines. Additional details can be found in **ref.** *12*.

because they are autofluorescent, but instead be tested in secondary assays that do not require fluorescence measurements (*see* **Subheading 3.4.; Fig. 3**).

3.3.4. Visual Inspection of Archived Images

A major benefit of image-based high-content analysis is the fact that images are retained after the scan and can be downloaded and visually inspected for the high-phosphorylation/low-phosphorylation phenotype described in the introduction. **Figure 5** shows representative

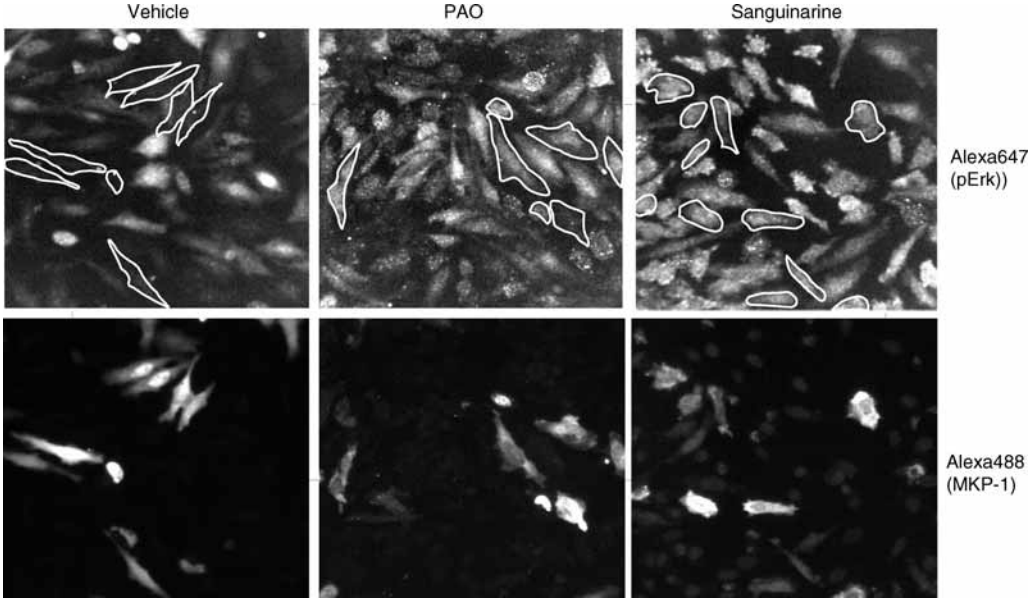

Fig. 5. Visual confirmation of a positive compound identified by chemical complementation assay with natural product library. Expression of nuclear phospho-Erk and MKP-1 were manually evaluated in archived immunofluorescence images acquired during the MKP-1 high content screen. Cells were identified by Hoechst 33342 staining. MKP-1 expression was determined on the basis of FITC (Alexa488) fluorescence (lower panels) and mapped onto phospho-Erk images acquired in the Cy5 (Alexa647) channel (top panels).

immunofluorescence images, in which MKP-1 expressing cells were identified on the basis of FITC (Alexa 488) fluorescence (lower panels) and mapped onto images acquired in the Cy5 (Alexa 647) channel (top panels). In the absence of small molecule compounds, MKP-1 expressing cells did not respond to TPA with increased Erk phosphorylation. Both the broad spectrum tyrosine phosphatase inhibitor, PAO, and one of the positive compounds in the MicroSource library, sanguinarine, restored Erk phosphorylation in the MKP-1 expressing cells, confirming the results from the 2D KS analysis. Visual confirmation of archived images also identifies image acquisition or analysis artifacts.

3.4. Secondary Assays

To illustrate the power of the chemical complementation assay for both primary and secondary assays, we compared the ability of sanguinarine to inhibit MKP-1 with a related phosphatase, MKP-3. HeLa cells were transfected with MKP-1 or MKP-3, treated, fixed, and stained, and single-cell contour plots were generated for each well as described in **Subheading 3.3.** The plate contained MKP-1 and MKP-3 transfected cells on the top half and the bottom half of the microplate. Wells A12:D12 were transfected with the phosphatase-inactive GFP, and wells E12:G12 and H12:L12 were transfected with MKP-1 or MKP-3, respectively, and treated with PAO. The graphical representation clearly shows high densities of phospho-Erk positive cells in GFP-expressing cell subpopulations and MKP-1 or MKP-3 expressing cell subpopulations that were treated with PAO. Wells that received sanguinarine show a concentration-dependent response in MKP-1 expressing cells but had little effect on MKP-3 expressing cells. The visual changes in cell population densities were then quantified using 2D KS statistics and produced concentration-response curves for inhibition of MKP-1 and MKP-3 by sanguinarine (**Fig. 6B**).

Other secondary assays are a Western blot implementation of the chemical complementation assay and in vitro assays using recombinant phosphatases, both of which have been described in

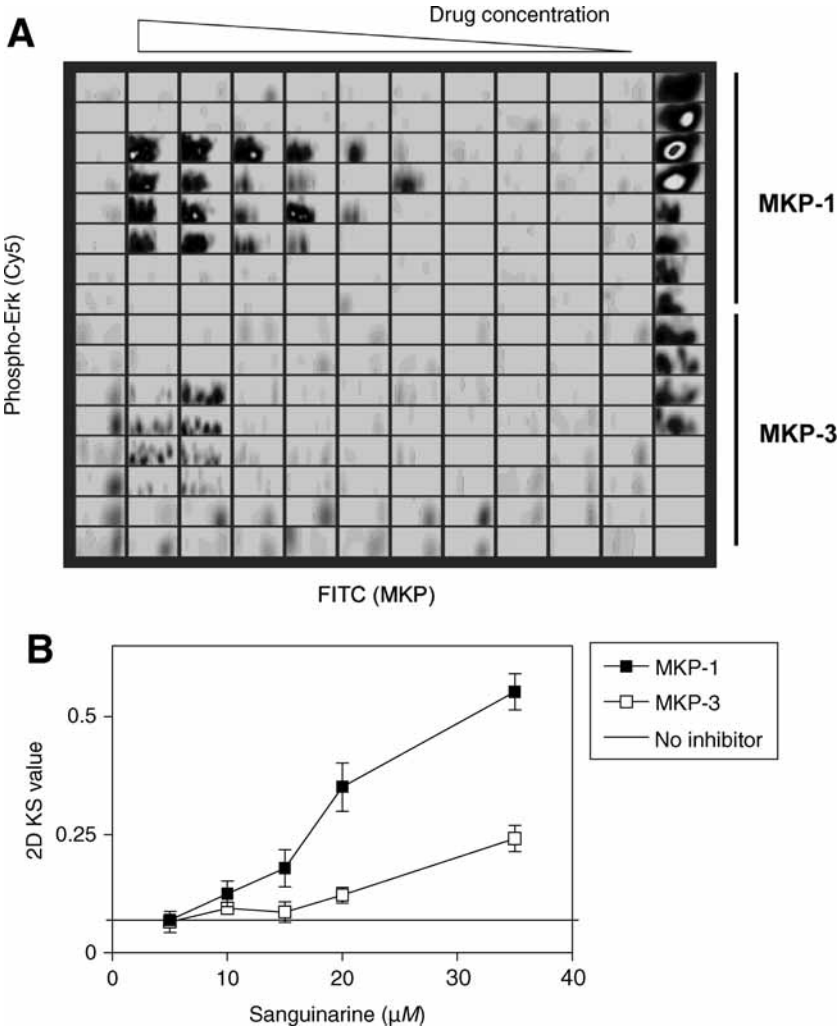

Fig. 6. Selective inhibition of MKP-1 but not MKP-3 by sanguinarine. **(A)** Single-cell density contour plots of phospho-Erk changes as a function of MKP-1 or MKP-3 expression in cells treated with different concentrations of sanguinarine. Cells transfected with MKP-1 are found in the upper portion of the panel, whereas those transfected with MKP-3 are shown in the lower portion of the panel. **(B)** Quantification of visual changes in cell population densities by 2D KS statistics.

detail *(10,12,20)*. Another option is surrogate readouts consistent with target inhibition. In the case of MKP inhibitors, this would encompass measurement of the phosphorylation status of MKP-1 target substrates, either by immunofluorescence or by Western blot analysis. This has been demonstrated in **ref.** *12* in which compounds with MKP-1 inhibitory activity activated the MKP-1 substrates Erk and JNK/SAPK.

3.5. Conclusions and Prospectus

Chemical complementation provides a potentially powerful tool to interrogate small molecules for their ability to interfere with specific molecular targets in intact cells. The strategy is especially useful when in vitro, target-based assays are not readily available, or in cases in which cellular phenotypic readouts are influenced by a multitude of factors. The approach is most

informative when the most proximal substrate of the target protein is used as an endpoint, as was illustrated with the Erk/MKP protein pair. Phenotypic readouts such as cell division, motility, shape, or DNA content, are subject to indirect effects.

The multiparametric version of chemical complementation should gain further utility if implemented in true high-throughput formats to screen diverse compound collections in intact mammalian cells. Preliminary results suggest that the assay can be robust enough for large-scale library screening *(12)*, however room for improvement remains.

For large-scale screening, it might be beneficial to develop cell lines that stably overexpress an intrinsically labeled form of the phosphatase of interest, perhaps with GFP, and use such constructs in coculture with the parental cell line. The assay in its current form requires a tightly timed incubation during stimulation with TPA. In principle, this step would not be required if cells could be identified that possess phospho-Erk levels high enough to be measured by immunofluorescence. To date, we have not been able to identify a cell line that shows constitutively high levels of nuclear phospho-Erk. Nonetheless, we believe the chemical complementation assay is the first definitive cell-based assay for phosphatase activity, and it appears reasonable to predict that in the near future a large-scale chemical complementation screen will identify potent, cell active inhibitors of phosphatase targets that are currently eluding drug discovery efforts.

4. Notes

1. We have found that Lipofectamine 2000 is best suited for high-throughput transfection followed by imaging. Other cationic lipids (Lipofectamine plus, Lipofectin) give fluorescent artifacts. Superfect (QIAGEN, Valencia, CA) also has low fluorescence artifacts but tended to give lower transfection efficiencies.
2. To perform data analysis on populations of single cells, we queried the Microsoft Access database produced by the BioApplication to extract single-cell average intensities in fluorescence channel 2 (FITC) and channel 3 (Texas Red or Cy5) by database query, followed by import into S-Plus for data manipulation and viewing. A useful means to quickly check the performance of an assay is the generation of a whole-plate trellis graph where Channel 2 and Channel 3 intensities are plotted on the *x*-axis and *y*-axis, respectively.
3. It is advisable to perform a visual check of transfection efficiency by manually counting the percentage of cells that appear green microscopically. The HCS platform allows the user to easily perform manual inspection of the images from which each set of cell features were extracted.

Acknowledgments

We thank Stephen Keyse and Nicholas Tonks for providing MKP-3 and MKP-1 expression plasmids, and Kenneth Giuliano for generating S-Plus scripts. This work was supported in part by NIH grants CA78039 and CA52995, and the Fiske Drug Discovery Fund.

References

1. Zolnierowicz, S. and Bollen, M. (2000) Protein phosphorylation and protein phosphatases. De Panne, Belgium, 19–24 September 1999. *EMBO J.* **19,** 483–488.
2. Tonks, N. K. and Neel, B. G. (2001) Combinatorial control of the specificity of protein tyrosine phosphatases. *Curr. Opin. Cell Biol.* **13,** 182–195.
3. Alonso, A., Sasin, J., Bottini, N., et al. (2004) Protein tyrosine phosphatases in the human genome. *Cell* **117,** 699–711.
4. Zou, X., Tsutsui, T., Ray, D., et al. (2001) The cell cycle-regulatory CDC25A phosphatase inhibits apoptosis signal-regulating kinase 1. *Mol. Cell Biol.* **21,** 4818–4828.
5. Chen, P., Hutter, D., Liu, P., and Liu, Y. (2002) A mammalian expression system for rapid production and purification of active MAP kinase phosphatases. *Protein Expr. Purif.* **24,** 481–488.
6. Slack, D. N., Seternes, O. M., Gabrielsen, M., and Keyse, S. M. (2001) Distinct binding determinants for ERK2/p38alpha and JNK map kinases mediate catalytic activation and substrate selectivity of map kinase phosphatase-1. *J. Biol. Chem.* **276,** 16,491–16,500.

7. Camps, M., Nichols, A., Gillieron, C., et al. (1998) Catalytic activation of the phosphatase MKP-3 by ERK2 mitogen-activated protein kinase. *Science* **280,** 1262–1265.
8. Balis, F. M. (2002) Evolution of anticancer drug discovery and the role of cell-based screening. *J. Natl Cancer Inst.* **94,** 78–79.
9. Vogt, A., Cooley, K. A., Brisson, M., Tarpley, M. G., Wipf, P., and Lazo, J. S. (2003) Cell-active dual specificity phosphatase inhibitors identified by high content screening. *Chem. Biol.* **10,** 733–742.
10. Vogt, A., Takahito, A., Ducruet, A. P., et al. (2001) Spatial analysis of key signaling proteins by high-content solid-phase cytometry in Hep3B cells treated with an inhibitor of Cdc25 dual-specificity phosphatases. *J. Biol. Chem.* **276,** 20,544–20,550.
11. Vogt, A. and Lazo, J. S. (2005) Chemical complementation: a definitive phenotypic strategy for identifying small molecule inhibitors of elusive cellular targets. *Pharmacol. Ther.* **107,** 212–215.
12. Vogt, A., Tamewitz, A., Skoko, J., Sikorski, R. P., Giuliano, K. A., and Lazo, J. S. (2005) The benzo (C) phenanthridine alkaloid, sanguinarine, is a selective, cell-active inhibitor of mitogen-activated protein kinase phosphatase-1. *J. Biol. Chem.* **280,** 19,078–19,086.
13. Young, I. T. (1977) Proof without prejudice: use of the Kolmogorov–Smirnov test for the analysis of histograms from flow systems and other sources. *J. Histochem. Cytochem.* **25,** 935–941.
14. Lampariello, F. (2000) On the use of the Kolmogorov–Smirnov statistical test for immunofluorescence histogram comparison. *Cytometry* **39,** 179–188.
15. Watson, J. V. (2001) Proof without prejudice revisited: immunofluorescence histogram analysis using cumulative frequency subtraction plus ratio analysis of means. *Cytometry* **43,** 55–68.
16. Cox, C., Reeder, J. E., Robinson, R. D., Suppes, S. B., and Wheeless, L. L. (1988) Comparison of frequency distributions in flow cytometry. *Cytometry* **9,** 291–298.
17. Giuliano, K. A., Chen, Y. T., and Taylor, D. L. (2004) High content screening with siRNA optimizes a cell biological approach to drug discovery: defining the role of P53 activation in the cellular response to anticancer drugs. *J. Biomol. Screen.* **9,** 557–568.
18. Peacock, J. A. (1983) Two-dimensional goodness-of-fit testing in astronomy. *Mon. Not. R. Astron. Soc.* **202,** 615–627.
19. Fasano, G. and Francescini, A. (1987) A multidimensional version of the Kolmogorov–Smirnov test. *Mon. Not. R. Astron. Soc.* **225,** 155–170.
20. Lazo, J. S., Aslan, D. C., Southwick, E. C., et al. (2001) Discovery and biological evaluation of a new family of potent inhibitors of the dual specificity protein phosphatase Cdc25. *J. Med. Chem.* **44,** 4042–4049.